Supplementary Figure S1

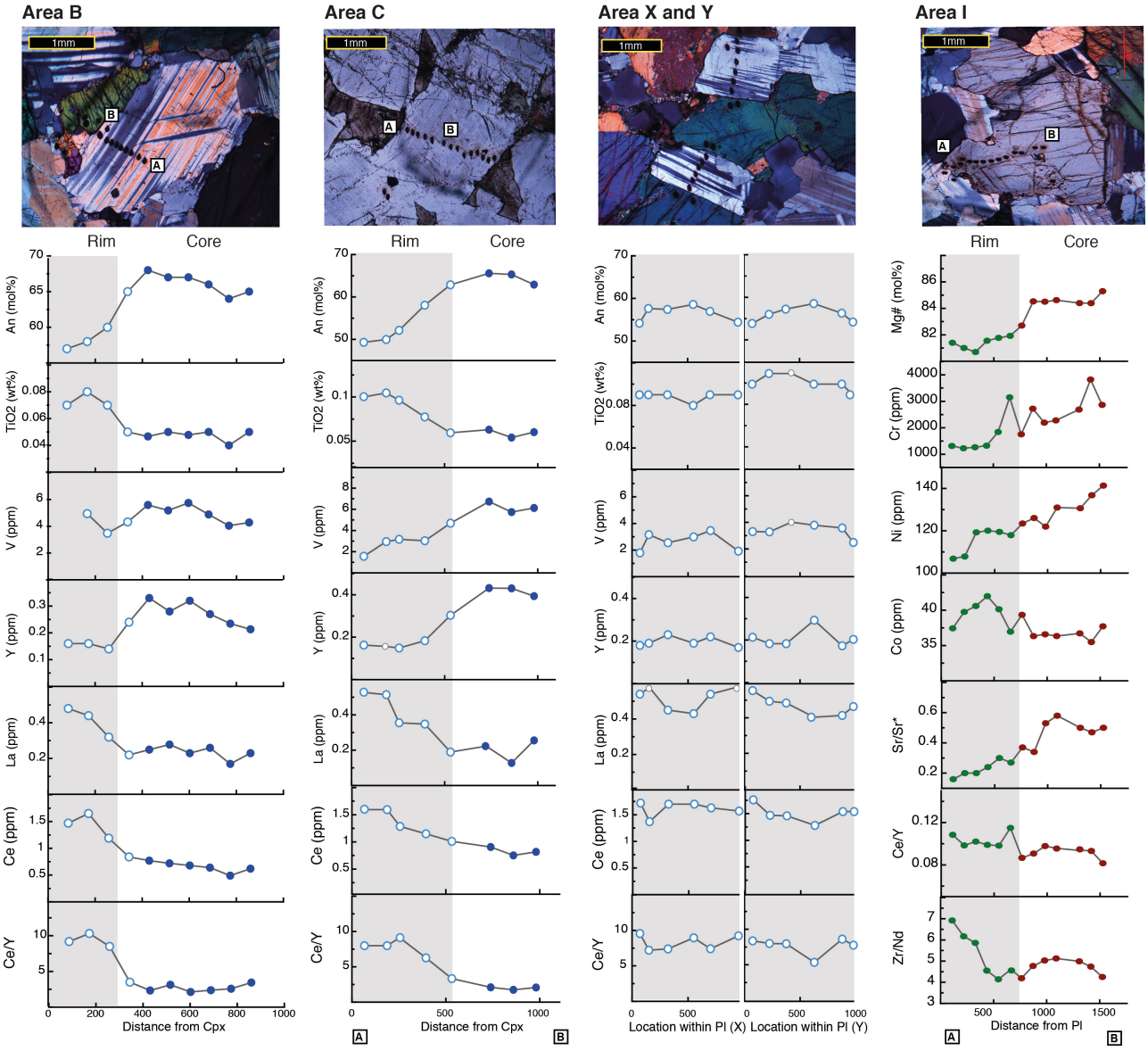

Figure S1. Plagioclase and clinopyroxene geochemical profiles of all grains selected (point B, C, X, Y and I). Plagioclase rim and clinopyroxene rim are defined on the chemical zoning and underlined by a grey background. Photomicrographs shows the locations of each point analyses.

Supplementary Figure S2

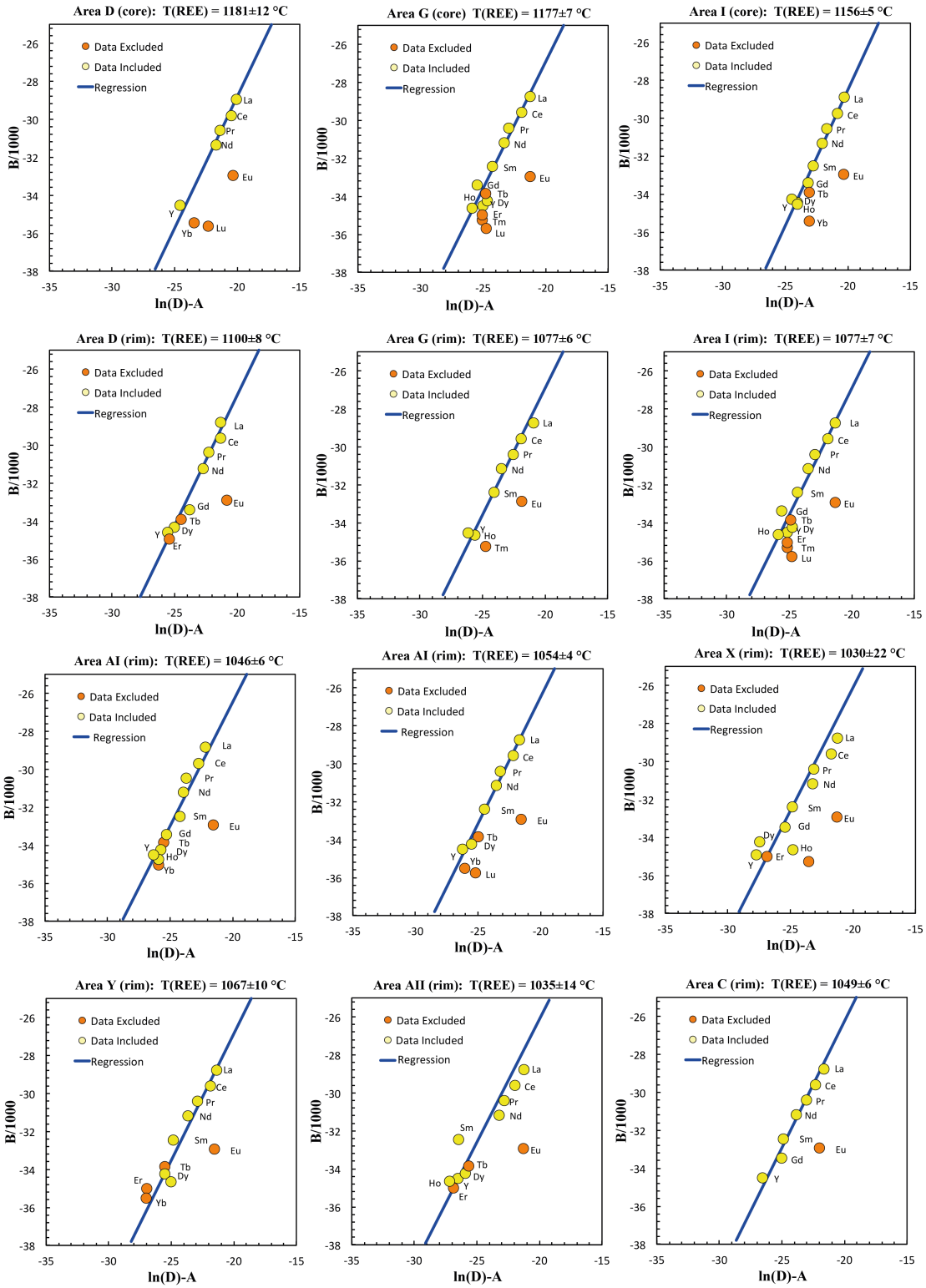

Figure S1. Ln(D)-A versus B/1000 diagrams for selected clinopyroxene-plagioclase couples in different areas of the thin section (see Fig.3), and relative equilibration temperatures calculated using the Cpx-Pl thermometer of Sun and Liang (2017). Eu, Tb, Er, Yb and Lu were excluded due to uncertainties in quantifications in plagioclase

Supplementary Figure S3

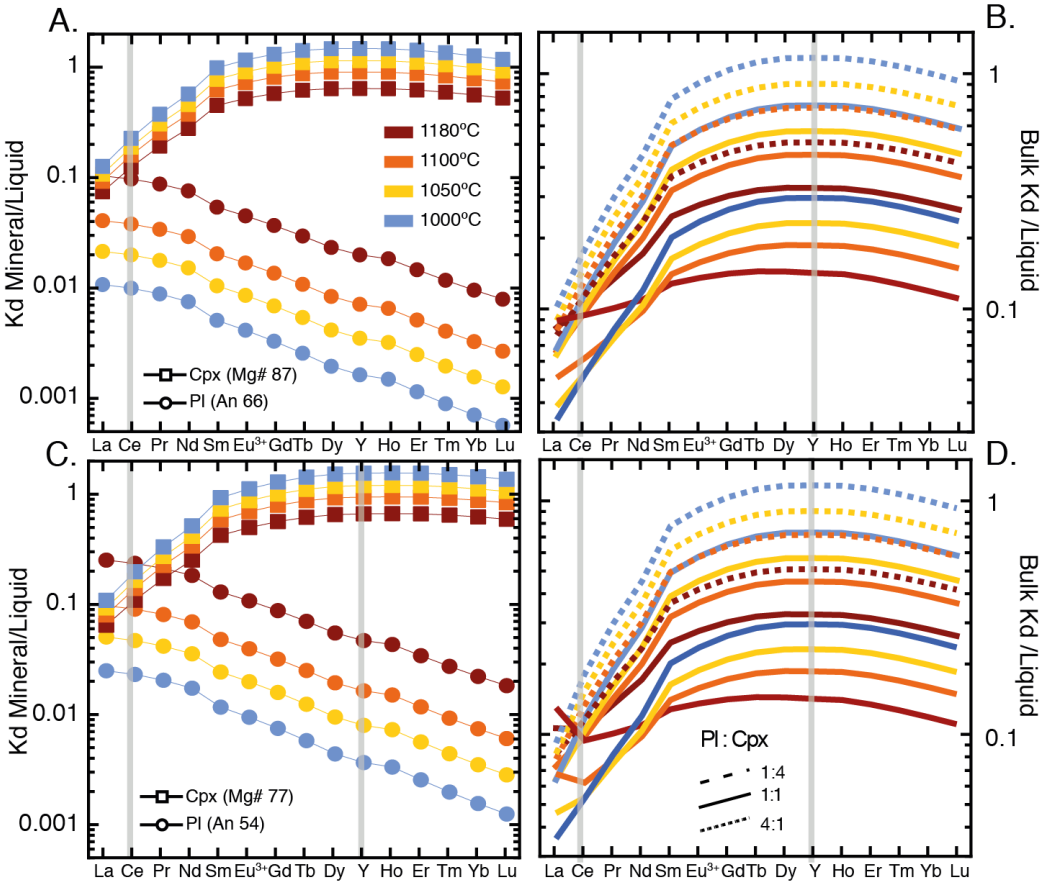

Figure S3. Effect of temperature and composition on REE-Y partitioning between clinopyroxene (Cpx) and plagioclase (Pl) and basaltic melts computed here on basis of Sun et al. (2017). A and C, variations in Kd mineral/liquid at temperature ranging from 1180ºC and 1000ºC for composition of Cpx- and Pl-I (A) and Cpx- and Pl-II (C). B and D, variations in bulk Kd at the same temperature and compositions of (A) and (B) and considering different Pl + Cpx assemblages. Note the different extent of variations in bulk Kd for Ce and Y, which may partly explain the more/less incompatible element fractionations observed in the recrystallised assemblage (see text).